Biochimica et Biophysica Acta 1818 (2012) 738–746

Contents lists available at SciVerse ScienceDirect

Biochimica et Biophysica Acta

journal homepage: www.elsevier.com/locate/bbamem

Effects of an antimalarial quinazoline derivative on human erythrocytes and on cell membrane molecular models

Yareli Rojas-Aguirre [a], Francisco Hernández-Luis [a], César Mendoza-Martínez [a], Carlos Patricio Sotomayor [b], Luis Felipe Aguilar [b], Fernando Villena [c], Ivan Castillo [d], David J. Hernández [d], Mario Suwalsky [c,*]

[a] Facultad de Química, Departamento de Farmacia, Universidad Nacional Autónoma de México, México, DF 04360, Mexico
[b] Instituto de Química, Pontificia Universidad Católica de Valparaíso, Valparaíso, Chile
[c] Faculty of Chemical Sciences, University of Concepción, Concepción, Chile
[d] Instituto de Química, Universidad Nacional Autónoma de México, Circuito Exterior, Ciudad Universitaria, México, DF 04360, Mexico

ARTICLE INFO

Article history:
Received 15 September 2011
Received in revised form 21 November 2011
Accepted 22 November 2011
Available online 3 December 2011

Keywords:
Malaria
Quinazoline derivative
Cyclodextrin
Inclusion complex
Erythrocyte membrane
Drug–membrane interaction

ABSTRACT

Plasmodium, the parasite which causes malaria in humans multiplies in the liver and then infects circulating erythrocytes. Thus, the role of the erythrocyte cell membrane in antimalarial drug activity and resistance has key importance. The effects of the antiplasmodial N^6-(4-methoxybenzyl)quinazoline-2,4,6-triamine (M4), and its inclusion complex (M4/HPβCD) with 2-hydroxypropyl-β-cyclodextrin (HPβCD) on human erythrocytes and on cell membrane molecular models are herein reported. This work evidences that M4/HPβCD interacts with red cells as follows: a) in scanning electron microscopy (SEM) studies on human erythrocytes induced shape changes at a 10 μM concentration; b) in isolated unsealed human erythrocyte membranes (IUM) a concentration as low as 1 μM induced sharp DPH fluorescence anisotropy decrease whereas increasing concentrations produced a monotonically decrease of DPH fluorescence lifetime at 37 °C; c) X-ray diffraction studies showed that 200 μM induced a complete structural perturbation of dimyristoylphosphatidylcholine (DMPC) bilayers whereas no significant effects were detected in dimyristoylphosphatidylethanolamine (DMPE) bilayers, classes of lipids present in the outer and inner monolayers of the human erythrocyte membrane, respectively; d) fluorescence spectroscopy data showed that increasing concentrations of the complex interacted with the deep hydrophobic core of DMPC large unilamellar vesicles (LUV) at 18 °C. All these experiments are consistent with the insertion of M4/HPβCD in the outer monolayer of the human erythrocyte membrane; thus, it can be considered a promising and novel antimalarial agent.

1. Introduction

Malaria is a disease caused by parasites of the genus *Plasmodium* spp. and it is transmitted via the bites of infected female *Anopheles* mosquitoes. *Plasmodium falciparum* and *Plasmodium vivax* are the prevalent species but the former is the most lethal. In the human body, parasites multiply in the liver, and then infect circulating erythrocytes where a cyclic asexual replication takes place bringing the cycles of fever and chills characteristic of malaria. If untreated, this infection can progress into severe illness often leading to death [1]. Malaria is endemic of tropical and subtropical regions, and approximately half of the world population lives at risk of this parasitic disease. With about 225 million of infected people and nearly 800,000 deaths in 2009, malaria is still considered one of the most severe diseases in the developing world [2]. Cure and prevention of malaria depend principally on drug therapy. Although several drugs have been commercialized, their use is now severely limited by the emergence and widespread of drug resistance. Furthermore, several reports indicate that these parasites have developed at least partial resistance to almost every antimalarial regimen introduced to date, including the former first-line drugs chloroquine and sulfadoxine–pyrimethamine [3–7]. Because of resistance, treatment failure is frequent, resulting in an increase of mortality and complicating the control of the infection. Therefore, there is an urgent need to gain information about the basic mechanisms through which antimalarial drugs act and resistance is generated in order not only to identify new targets and develop new drugs with novel mechanisms of action, but also to take advantage of the mode of action of available drugs and make better use of them [6,7]. An extensively studied target has been the inhibition of folate metabolism. The antifolate drugs used for malaria therapy are

Abbreviations: SEM, scanning electron microscopy; IUM, isolated unsealed erythrocyte membrane; RBCS, red blood cell suspensions; LUV, large unilamellar vesicles; DMPC, dimyristoylphosphatidylcholine; DMPE, dimyristoylphosphatidylethanolamine; r, fluorescence anisotropy; GP, general polarization; DPH, 1,6-diphenyl-1,3,5-hexatriene; laurdan, 6-dodecanoyl-2-dimethylaminonaphtalene; PfDHFR, dihydrofolate reductase; M4, N^6-(4-methoxybenzyl)quinazoline-2,4,6-triamine; CDs, cyclodextrins; HPβCD, 2-hydroxypropyl-β-cyclodextrin

* Corresponding author. Tel.: +56 41 2204171; fax: +56 41 2245974.
E-mail address: msuwalsk@udec.cl (M. Suwalsky).

0005-2736/$ – see front matter © 2011 Elsevier B.V. All rights reserved.
doi:10.1016/j.bbamem.2011.11.026

sulfadoxine, which inhibits the dihydropteroate synthetase enzyme (PfDHPS), and pyrimethamine, which inhibits dihydrofolate reductase (PfDHFR) activity of the bifunctional dihydrofolate reductase/thymidylate synthase enzyme, essential systems for parasitic DNA synthesis. The drug combination sulfadoxine–pyrimethamine (Fansidar) was introduced in the 70s after the emergence of parasite resistance to chloroquine. It used to be a highly effective, affordable, and well-tolerated drug combination until the emergence of resistant parasites [7]. Numerous efforts have been directed toward the discovery of new PfDHFR inhibitors, being quinazoline derivatives the most promising compounds [8–12].

Pharmacological activity of a drug frequently involves an initial interaction with cell membranes, even if they are not the final targets. Given the important role of the erythrocytes host cell membrane on drug resistance, more investigation about antimalarial drug–membrane interaction is needed. In this context, it was decided to study N^6-(4-methoxybenzyl)quinazoline-2,4,6-triamine, synthesized in the 70s as a promising PfDHFR inhibitor. Its synthesis and antiplasmodial activity were initially described, but the investigation was apparently abandoned [8]. This quinazoline derivative, named in this work as M4 (Fig. 1), was used to investigate its interaction with human erythrocytes and cell membrane molecular models in order to have an understanding, at both cellular and molecular levels about the relation between the compound and the erythrocyte membrane. When M4 was synthesized according to the described procedure [8], it showed poor aqueous solubility but high solubility in dimethylsulfoxide (DMSO), an organic solvent widely employed in pre-formulations of new compounds in biological trials. However, investigations have shown that DMSO does exert a direct effect on the major characteristics of model membranes [13], which could potentially hinder this work. To overcome these drawbacks, increasing the aqueous solubility of M4 was of importance and this was achieved through the formation of an inclusion complex with a modified cyclodextrin. Cyclodextrins (CDs) are cyclic oligomers formed by glucopyranose molecules bound through 1–4 bonds, and are most commonly composed by 6 (α-CD), 7 (β-CD) or 8 (δ-CD) glucose units. CDs are able to form inclusion complexes with different classes of molecules, modifying their physical, chemical and biological properties [14]. Among CDs, 2-hydroxypropyl-β-cyclodextrin (HPβCD) appears to be especially useful given its low toxicity, complexation potential and great water solubility [15,16]. Thus, the inclusion complex of M4 with HPβCD (M4/HPβCD) was prepared in order to study the interaction of the quinazoline derivative with membrane phospholipids circumventing the use of DMSO. The characterization of the complex consisted on phase solubility studies, nuclear magnetic resonance and mass spectrometry experiments. Afterwards, the interaction of M4/HPβCD with human red blood cells and molecular models of the erythrocyte membrane was carried out. The influence of M4/HPβCD on morphology of intact human erythrocytes was examined by scanning electron microscopy (SEM), while isolated unsealed human erythrocyte membranes (IUM) were studied by fluorescence spectroscopy. Molecular models consisted of bilayers of dimyristoylphosphatidylcholine (DMPC) and dimyristoylphosphatidylethanolamine (DMPE), representative of phospholipid classes located in the outer and inner monolayers of the human erythrocyte membrane, respectively [17,18]. The capacity of M4/HPβCD to perturb the bilayer structures of DMPC and DMPE was assessed by X-ray diffraction while DMPC large unilamellar vesicles (LUV) were additionally studied by fluorescence spectroscopy.

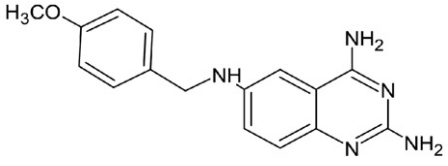

Fig. 1. Structure formula of N^6(4-methoxybenzyl)quinazoline-2,4,6-triamine (M4).

2. Materials and methods

2.1. X-ray structure determination of M4

M4 single crystals were mounted at 123 K on a Bruker SMART diffractometer equipped with an Apex CCD area detector. Frames were collected by omega scans, and integrated with the Bruker SAINT software package using the appropriate unit cell [19]; the structure was solved using the SHELXS-97 program [20] and refined by full-matrix least-squares on F^2 with SHELXL-97 [21]. Weighted R-factors, R_w, and all goodness of fit indicators, S, were based on F^2. The observed criterion of ($F^2 > 2\sigma F^2$) was used only for calculating the R-factors. All non-hydrogen atoms were refined with anisotropic thermal parameters in the final cycles of refinement. Hydrogen atoms were placed in idealized positions. Isotropic thermal parameters of the hydrogen atoms were assigned the values of $U_{iso} = 1.2$ times the thermal parameters of the parent non-hydrogen atom. Data: Mol. wt. = 608.71, triclinic, space group *P*-1, $a = 10.3555(15)$ Å, $b = 11.4769(16)$ Å, $c = 13.8216(19)$ Å, $\alpha = 92.356(3)^o$, $\beta = 111.367(3)^\circ$, $\gamma = 102.190(3)^\circ$, $V = 1482.7(4)$ Å^3. $T = 123(2)$ *K*, $Z = 2$, $D_{calc} = 1.363$ g cm^{-3}, $\mu = 0.092$ mm^{-1}, 5492 Reflections collected, 5492 independent ($R_{int} = 0.0393$), final R_1 [$I \geq 2\sigma(I)$] = 0.0439, $wR(F^2) = 0.1006$, $S = 1.052$.

2.2. Preparation of the inclusion complex

The inclusion complex was obtained by mixing M4 and HPβCD in water at 1:1 molar ratio. The mixture was stirred at 25 °C for 7 days protected from light to prevent degradation. After this period, the solvent was evaporated to dryness at 45 °C under vacuum (Vacuubrand CVC2^{II}). The resulting solid was collected, pulverized and sieved (200 μm sieve).

2.3. Determination of intrinsic solubility

The intrinsic solubility of M4 and the solubility profile of M4/HPβCD were determined by the shake-flask method [22]. Briefly, an aliquot of 5 ml of phosphate buffer solution, pH 7.4, was added to a glass vial containing 5 mg of M4 or its mass equivalent as a complex in order to have an excess of solid. The vials were stirred during 48 h at 25 °C followed by a sedimentation period of 18 h for phase separation. The amount of dissolved compound was analyzed by UV spectrophotometry at 290 nm (Genesys10uv, Thermo). Three independent experiments were carried out.

2.4. Phase solubility diagram

In order to determine the effect of HPβCD on the solubility of M4, phase solubility studies were performed according to the method described by Higuchi and Connors [23]. Briefly, aqueous solutions containing increasing concentrations of HPβCD were prepared (0.2, 0.4, 0.6, 0.8 and 1 mM). A constant amount of M4 in five-fold molar excess relative to the highest concentration of HPβCD solution was added to the HPβCD solution; the resulting suspensions were stirred during 48 h at room temperature. After this period, the suspensions were filtered through 0.2 μm membranes (Millex, Millipore) and M4 concentration was analyzed by means of an UV spectrophotometer at 290 nm (Genesys10uv, Thermo). Phase solubility diagrams were obtained by plotting M4 solubility versus HPβCD concentration. This experiment was repeated three times.

2.5. NMR spectroscopy

^{1}H and ROESY NMR spectra were obtained from a Bruker Avance III spectrometer at 400 MHz; samples of M4 were referenced relative to the residual protons of DMSO-d_6 at δ 2.50 ppm. ROESY spectra were acquired with a mixing time of 200 ms.

2.6. ESI-mass spectrometry

Electrospray mass spectrometry experiments were performed with a Bruker Daltonics Esquire 6000 spectrometer with ion trap; data were collected from ca. 5 mM 1:1 M4/HPβCD aqueous solutions.

2.7. Scanning electron microscopy (SEM) studies of human erythrocytes

The interaction of M4/HPβCD with human erythrocytes was studied in vitro according to the following procedure. Five blood drops from a non medicated human healthy donor were obtained by puncturing the ear lobule and placed in an Eppendorf tube containing 10 μl of heparin (5000 UI/ml) in 900 μl of saline solution (0.9% NaCl, pH 7.4); the tube was mixed manually and then centrifuged (1000 rpm for 10 min); the supernatant was discarded and replaced by the same volume of saline solution; the whole process was repeated three times. The sedimented erythrocytes were suspended in 900 μl of saline solution, and 100 μl of this suspension was mixed with equal volumes of either saline solution (control) or 100 μl of the adequate M4/HPβCD stock saline solutions to obtain the final concentrations of 10, 50, 100, 150, 200 and 250 μM (relative to M4). In vitro interactions of HPβCD (250 μM) and free M4 (as an aqueous suspension ca. 250 μM) with red blood cells were also evaluated. Samples were incubated at 37 °C for 1 h. After this period samples were centrifuged at 1000 rpm for 10 min and the supernatant was discarded. To fix the erythrocytes, 500 μl of 2.5% glutaraldehyde was added to each sample followed by incubation at 4 °C overnight. Fixed cells were washed with distilled water, and directly placed over Al glass cover stubs, air-dried at 37 °C for 30 min, and gold-coated for 3 min at 10^{-1} Torr in a sputter device (Edwards S150, Sussex, England). Resulting specimens were examined in a Jeol SEM (JSM 6380 LB, Japan).

2.8. Fluorescence measurements of DMPC large unilamellar vesicles (LUV) and of isolated unsealed human erythrocyte membranes (IUM)

The influence of M4/HPβCD on the physical properties of DMPC LUV and IUM was studied by fluorescence spectroscopy using DPH (1,6-diphenyl-1,3,5-hexatriene) fluorescent probe (Molecular Probes, Invitrogen, Carlsbad, CA). DMPC large unilamellar vesicles (LUV) suspended in water were prepared by extrusion of frozen and thawed multilamellar liposome suspensions (final lipid concentration 0.4 mM) through two stacked polycarbonate filters of 400 nm pore size (Nucleopore, Corning Costar Corp., MA, USA) under nitrogen pressure at 10 °C above the lipid phase transition temperature. Erythrocytes were separated from heparinized venous blood samples obtained from regular non-medicated casual donors by centrifugation and washing procedures. IUM were prepared by lysis, according to Dodge et al. [24]. DPH was incorporated into DMPC LUV and IUM suspensions by addition of adequate aliquot of 0.5 mM solution of the probe in DMSO in order to obtain a final concentration of 1×10^{-3} mM. Afterwards, the suspensions were incubated at 37 °C for 1 h. Steady state and time-resolved fluorescent measurements were performed on a K2 multifrequency phase shift and modulation spectrofluorometer (ISS Inc., Champaign, IL, USA) interfaced to computers. Software from ISS was used for data collection and analysis. The exciting light was from a modulable ISS 375 nm Light Emitting Diode (LED) laser. M4 and M4/HPβCD were incorporated into LUV suspensions by addition of adequate aliquots of a stock solution of M4 or M4/HPβCD (250 μM in a water-DMSO 50:50 mixture) in order to get the final concentrations used in these experiments (1–10 μM, where the maximum of DMSO was 0.2%). Samples were then incubated at 37 °C for ca. 15 min and measured at two different temperatures by means of 5 mm path-length square quartz cuvettes: 18 °C because the X-ray experiments were performed at this temperature and 37 °C because that is the normal physiological temperature. Sample temperature was controlled by an external bath circulator (Cole-Parmer, Chicago, IL, USA) and monitored before and after each measurement using an Omega digital thermometer (Omega Engineering Inc., Stanford, CT, USA). Anisotropy measurements were made in the L configuration using Glan–Thompson prism polarizers (ISS) in both exciting and emitting beams. The emission was measured using a WG-420 Schott high-pass filter (Schott WG-420, Mainz, Germany) with negligible fluorescence. Blank subtraction was performed in all measurements using unlabeled samples without probes. The acquired results represent mean values and standard error of ten measurements in two independent samples. Unpaired Student's *t*-test was used for statistical calculations. DPH fluorescence anisotropy (r) was calculated according to the definition: $r=(I_{||}-I_{\perp})/(I_{||}+2I_{\perp})$ where $I_{||}$ and $I_{\perp}$ are the corresponding vertical and horizontal emission fluorescence intensities with respect to the vertically polarized excitation light [25]. In addition, the definition of the average anisotropy of a mixture of fluorophors was used to determine the value of DPH anisotropy. In the experimental conditions there were two species that have fluorescence properties: M4 and DPH probe. The average anisotropy for a mixture of fluorophors is given by: $\bar{r}=\sum_i f_i r_i$, where f_i is the fraction of intensity for each species, and r_i is the anisotropy for each component of the mixture. Thus the anisotropy of DPH was calculated by the equation: $\bar{r}=f_{DPH}r_{DPH}+f_{M4}r_{M4}$.

For fluorescence decay determination, lifetime measurements were performed with the polarizers oriented in the "magic angle" condition [26]. Phase and modulation values were obtained at ten modulation frequencies (5–80 MHz) as previously described [27]. Dimethyl-POPOP (1,4-bis[2]4-Methyl-5-phenyloxazoly benzene) in ethanol ($t=1.45$ ns) was used as a reference of intensity decay. Time-resolved fluorescence intensity decay data of DPH was analyzed using a Lorentzian lifetime distribution. A fixed discrete lifetime component of 0.01 ns was used to account for scattered light, which was <2% in terms of fractional intensity contribution. The Lorentzian lifetime distribution center obtained from the analysis is informed as DPH lifetime.

2.9. X-ray diffraction studies of phospholipid multilayers

The capacity of the M4/HPβCD complex to perturb the structures of DMPC and DMPE multilayers was evaluated by X-ray diffraction. Synthetic DMPC (lot 140PC-248, MW 677.9) and DMPE (lot 140PE-58, MW 635.9) from Avanti (ALA, USA), were used without further purification. Approximately 2 mg of each phospholipid were mixed in Eppendorf tubes with 200 μl of (a) distilled water or (b) aqueous solutions of M4/HPβCD in the range of concentrations of 1 to 250 μM (relative to M4); free M4 was evaluated as a suspension at ca. 250 μM. The mixtures were incubated during 30 min at 37 °C and 60 °C with DMPC and DMPE respectively, and centrifuged for 10 min at 2500 rpm. Samples were then transferred to 1.5 mm diameter special glass capillaries (Glas-Technik & Konstruktion, Berlin, Germany) and X-ray diffracted utilizing Ni-filtered Cu-Kα radiation from a Bruker Kristalloflex 760 (Karlsruhe, Germany) X-ray system. Specimen-to-film distances were 8 and 14 cm, standardized by sprinkling calcite powder on the capillary surface. Relative reflection intensities were obtained in an MBraun PSD-50 M linear position-sensitive detector system (Garching, Germany); no correction factors were applied. The experiments were performed at 18 °C ± 1 °C, which is below the main phase transition temperature of both phospholipids. Higher temperatures would have induced transitions to further fluid phases making the detection of structural changes more difficult. Each experiment was performed by triplicate. X-ray data were analyzed using the Origin software 7.0.

3. Results

3.1. X-ray crystallography

The solid-state structure of M4 was determined by single-crystal X-ray diffraction in order to confirm its identity, and also to determine the spatial arrangement of the aromatic rings; yellow-orange plates were grown from an approximately 1:1 water/ethanol concentrated

solution of M4 by slow evaporation. Crystallographic data reveal that there are two independent molecules in the asymmetric unit with virtually identical parameters, except for the non-coplanar angles between the phenyl and quinazoline rings in each molecule, which correspond to 68.54 and 59.52° for molecules A and B (Fig. 2). An extended hydrogen-bond network stabilizes the lattice, involving intermolecular N–H···N base pairing, as well as N–H···O (methoxy) and N···H–O (water) interactions (Table 1). The bond lengths and angles are similar to those for related quinazoline derivatives [28,29].

3.2. Determination of intrinsic solubility

The aqueous solubility of M4 and M4/HPβCD is presented in Table 2. According to these results, the improvement of M4 solubility in water through the formation of an inclusion complex with HPβCD increased 10.4 times.

3.3. Phase solubility diagram

Fig. 3 shows a solubility curve that can be classified as A_L type diagram, which indicates that there is a linear increase in M4 solubility with increasing concentrations of HPβCD. This result is indicative of the formation of a soluble complex between M4 and this cyclodextrin [23]. Because such profile is characterized by a slope of less than 1, it was assumed that the solubility increase was due to the formation of a 1:1 complex [23]. From the straight line of the phase-solubility diagram the apparent stability constant ($K_{1:1}$) was estimated according to the equation $K_{1:1} = m/So(1-m)$, where m is the slope of the linear plot and So is M4 aqueous solubility ($So = 0.00935$ mg/ml, 0.0000316 M) determined as described above. The value of $K_{1:1}$ is a useful index to estimate the degree of binding strength of the complex. The magnitude of $K_{1:1}$ is generally in the range 0–100,000 M^{-1} with 0 being the value for a drug that is incapable of forming an inclusion complex; values less than 100 M^{-1} denote weak guest–host associations, whereas values close to 10,000 M^{-1} indicate strong interactions, and 100,000 M^{-1} being near the upper value observed experimentally for cyclodextrin complexes of drugs [30]. The $K_{1:1}$ value for the M4/HPβCD inclusion complex was 2765 M^{-1}, suggesting that there is a favorable interaction between the quinazoline derivative and the cyclodextrin.

3.4. ^{1}H NMR spectroscopy

The inclusion mode of M4 with the cyclodextrin was examined by NMR spectroscopy. Due to the poor solubility of M4 in water, its ^{1}H NMR spectrum was acquired in DMSO-d_6. The aliphatic signals at δ 3.65 and 4.17 ppm were assigned to CH_3O- and $-CH_2NH-$ protons, with relative intensities of 3 H and 2 H, respectively. The aromatic region is characterized by the presence of two doublets corresponding to the coupled protons in the disubstituted phenyl ring at δ 6.82 and 7.27 ppm ($J = 10.6$ Hz). A singlet at δ 6.86 ppm overlaps with the former doublet, giving rise to an apparent multiplet that integrates to 3 H; in addition, a broad singlet at δ 7.05 ppm corresponding to two protons of the quinazoline ring gives a total of 7 aromatic protons, as expected for M4. Detailed information on the inclusion of M4 within the cavity of HPβCD was obtained from 2D NMR experiments, specifically with Rotating-frame NOE spectroscopy (ROESY). The 2D spectrum of the M4/HPβCD system was acquired in DMSO-d_6; the ROESY contour plot reveals that the doublet corresponding to the phenyl ring at δ 6.82 ppm has a strong intermolecular cross-peak with H-3 on the wide side of the cavity of HPβCD at δ 3.65 ppm (Fig. 4). This indicates that M4 forms an inclusion complex through its 4-methoxyphenyl group with the cyclodextrin in DMSO, result that agrees with the phase-solubility diagram in aqueous solution.

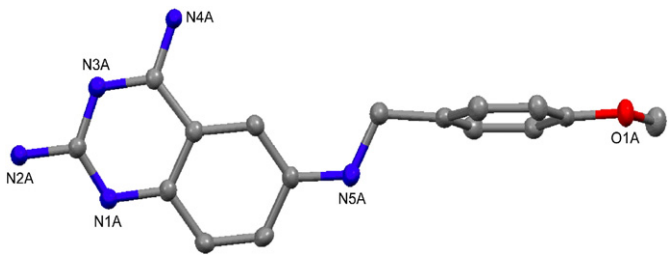

Fig. 2. ORTEP diagram of one of the independent molecules (A) of M4 at the 50% probability level with atom labeling scheme; hydrogen atoms and a water molecule were removed for clarity.

Table 1
Hydrogen bonding parameters (Å, °) for M4.

D–H···A	Symmetry operation	D–H	H···A	D···A	D–H···A
N4B–H44···O1A	−x, 1−y, −z	0.876	2.253	2.984	140.85
N4A–H42···O1B	−x, 1−y, −z	0.894	2.251	2.989	139.72
N4B–H43···N3A	1−x, 2−y, 1−z	0.879	2.175	3.014	159.39
N4A–H41···N3B	1−x, 2−y, 1−z	0.899	2.125	3.019	172.77
N2B–H24···N1A	2−x, 2−y, 1−z	0.878	2.082	2.959	177.96
N2A–H22···N1B	2−x, 2−y, 1−z	0.892	2.139	3.026	172.71
O2–H26···N1A	2−x, 2−y, 1−z	0.877	2.142	2.985	161.18
O2–H25···N1B		0.878	2.158	3.002	161.24

3.5. Mass spectrometry

Electrospray (ESI) mass spectrometry experiments revealed a distribution of peaks between m/z = 1180 and 2000; the ones between m/z = 1215.5 and 1737.8 are associated to sodium cationized HPβCD with varying degrees of substitution with hydroxypropyl groups (Fig. 5). The peaks at m/z = 1778.8, 1836.9 and 1895.9 correspond to the inclusion complexes $[M4+(6)+H]^+$, $[M4+(7)+H]^+$, and $[M4+(8)+H]^+$, respectively; the number in parenthesis represents the number of hydroxypropyl substituents on the cyclodextrin. These experimental data are consistent with predominant inclusion compounds with 1:1 stoichiometry.

3.6. Scanning electron microscopy (SEM) studies of human erythrocytes

The effects of the interaction of M4 and M4/HPβCD with human erythrocytes were evaluated in vitro by SEM. The resulting micrographs (Fig. 6) show that the inclusion complex induced notorious changes in the morphology of the red blood cells. The normal resting shape of the human red blood cell is a flattened biconcave disc shape (discocyte) ~8 μm in diameter which can be observed in Fig. 6A, corresponding to the erythrocytes incubated with saline solution (control). On the other hand, morphological analysis of the results revealed that M4/HPβCD changed the normal shape of the red blood cells in a dose-dependent manner. Fig. 6B (10 μM) clearly shows that discocytes underwent a transformation to class I echinocytes, which are erythrocytes with crenated shapes [31]; nevertheless knizocytes (term designating a triconcave red-cell shape) were present as well. M4/HPβCD at 100 μM gave rise to echinocytosis phenomenon with the presence of class III echinocytes (quasi spherical body covered with round

Table 2
Solubility of M4 and its M4/HPβCD complex.

Compound	Solubility (mg/ml) (mean ± SD)	$^a S_{CD}/^b S_{M4}$
M4	0.00935 ± 0.00035	–
M4/HPβCD	0.0976 ± 0.00451	10.4

[a] S_{CD}: M4/HPβCD complex solubility.
[b] S_{M4}: M4 solubility.

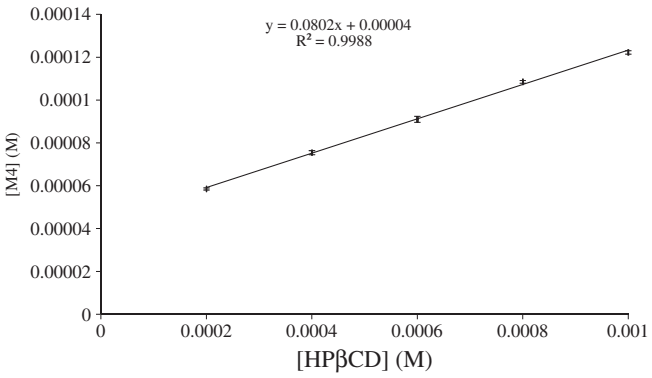

Fig. 3. Phase-solubility diagram for M4/HPβCD host–guest system at 25 °C.

protuberances) [31], although some knizocytes and stomatocytes (erythrocytes with cup-like shapes) were also found (Fig. 6C). Cellular polymorphism was produced at 250 μM, where the presence of echinocytes, knizocytes, stomatocytes and ellyptocytes (abnormally shaped elongated red blood cells) was evident (Fig. 6D). The effects of the separate components were also studied. Minor cell transformation was induced by HPβCD, although some stomatocytes and knizocytes were present (Fig. 6E). In the case of free M4 (Fig. 6F) echinocytes were the dominating shape. The quinazoline derivative also produced some knizocytes and stomatocytes. Very few discocytes were observed. Thus, SEM observations evidenced that M4/HPβCD affected human erythrocytes in all range of concentrations and induced predominantly the formation of echinocytes.

3.7. Fluorescence measurements of DMPC large unilamellar vesicles (LUV) and of isolated unsealed human erythrocyte membranes (IUM)

DPH, an extrinsic membrane probe, was used because of its favorable spectral properties for the phospholipids deep hydrophobic acyl chain region. Lipid acyl chain packing order and water penetration changes were obtained from steady state and time resolved fluorescence measurements. Steady state DPH fluorescence anisotropy changes due to the interactions of free M4 and M4/HPβCD with the deep hydrophobic core of DMPC LUV are depicted in Fig. 7. These results show that increasing concentrations of free M4 or M4/HPβCD substantially decreased the anisotropy values at 18 °C. Similarly, there was a moderate decrease of anisotropy at 37 °C, when the lipid bilayer is in the liquid-crystalline state. Fig. 8 shows the effect on DPH anisotropy at 37 °C of M4 and M4/HPβCD in IUM. As it can be appreciated, a concentration as low as 1 μM of each compound induced sharp anisotropy decrease where the major change occurred upon the addition of this concentration, with subsequent slight decreases at higher concentrations. Fig. 9 shows that increasing M4 and M4/HPβCD concentrations produced a monotonically decrease of DPH lifetime in IUM at 37 °C; however, increasing amounts of the free compound and the complex did not show a significant effect on the DPH lifetime in DMPC LUV at both studied temperatures (data not show).

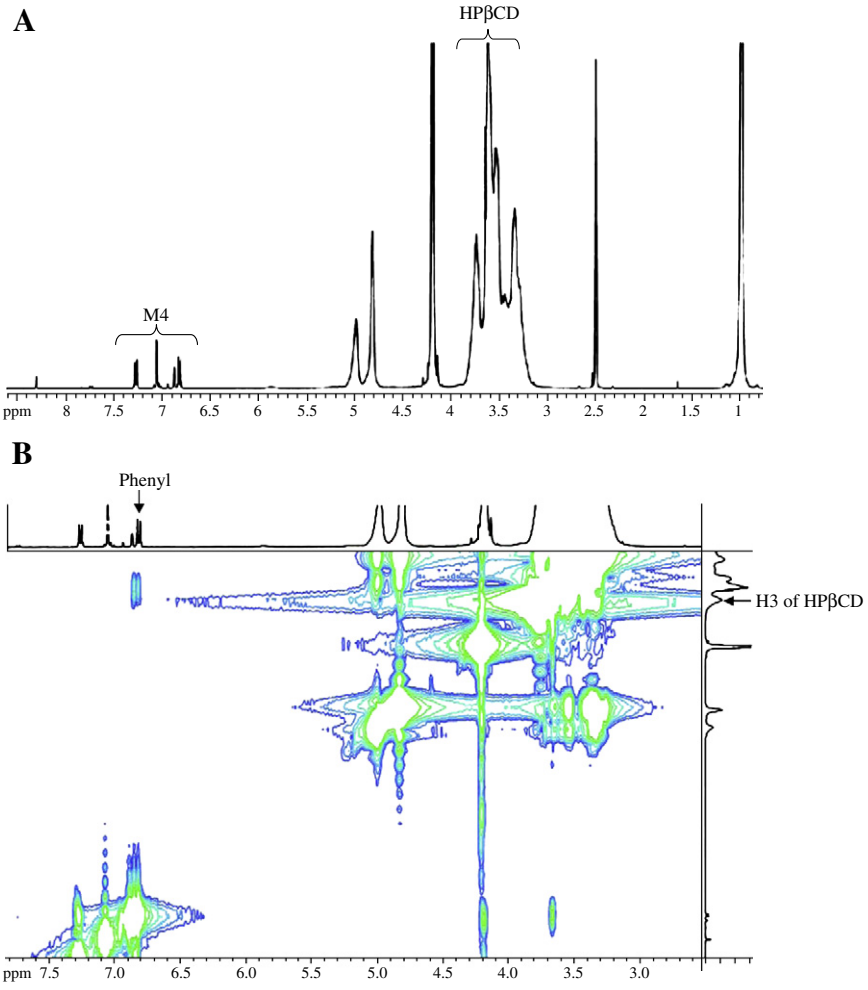

Fig. 4. ^{1}H NMR (A) and ROESY spectra (B) of M4/HPβCD.

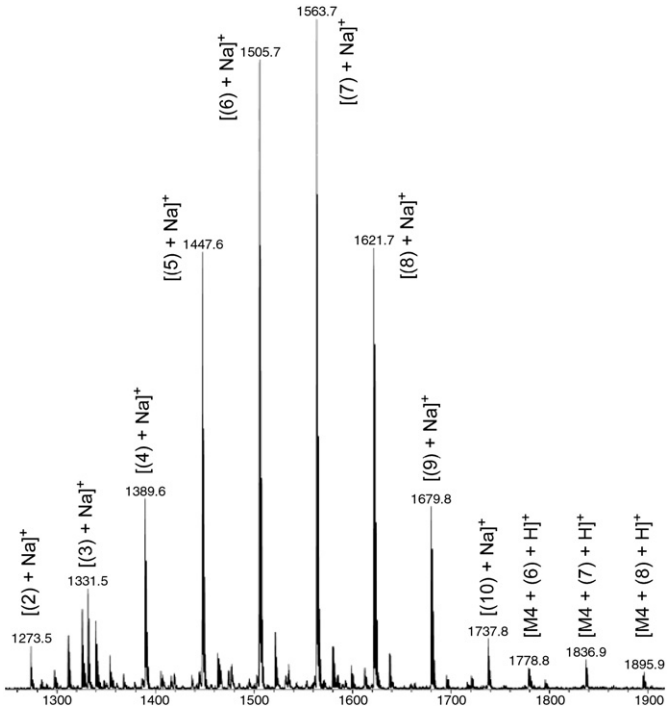

Fig. 5. Electrospray mass spectrum of M4/HPβCD aqueous solution; numbers shown in brackets refer to the number of hydroxypropyl groups bound to cyclodextrin.

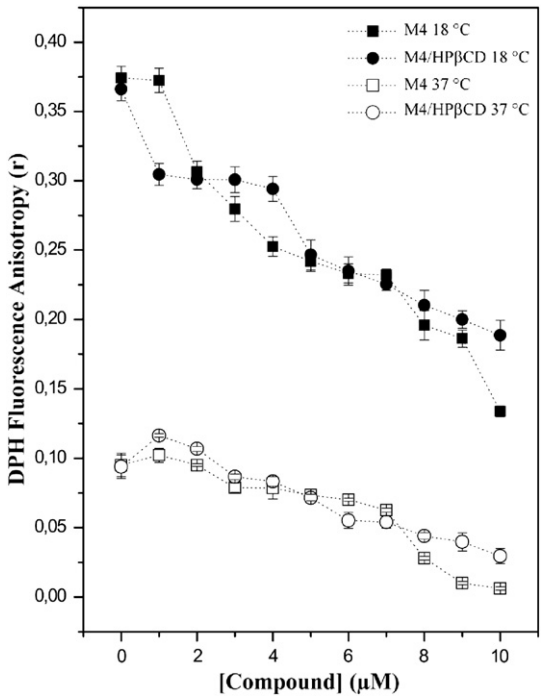

Fig. 7. Effect of M4/HPβCD and M4 on the steady state fluorescence anisotropy of DPH in DMPC LUV at 18 °C and 37 °C.

3.8. X-ray diffraction studies of phospholipid multilayers

Fig. 10A exhibits the results obtained by incubating DMPC with water, M4/HPβCD, free M4 and HPβCD. As expected, water altered the structure of DMPC; its bilayer repeat distance (phospholipid bilayer width plus the layer of water) increased from about 55 Å in its crystalline form to 64.5 Å when immersed in water, and its low-angle reflections (indicated as LA) were reduced to only the first two orders of the bilayer repeat [32]. On the other hand, only one strong reflection of 4.2 Å showed up in the wide-angle region (indicated as WA), which corresponds to the average distance between fully extended acyl chains organized with rotational disorder in

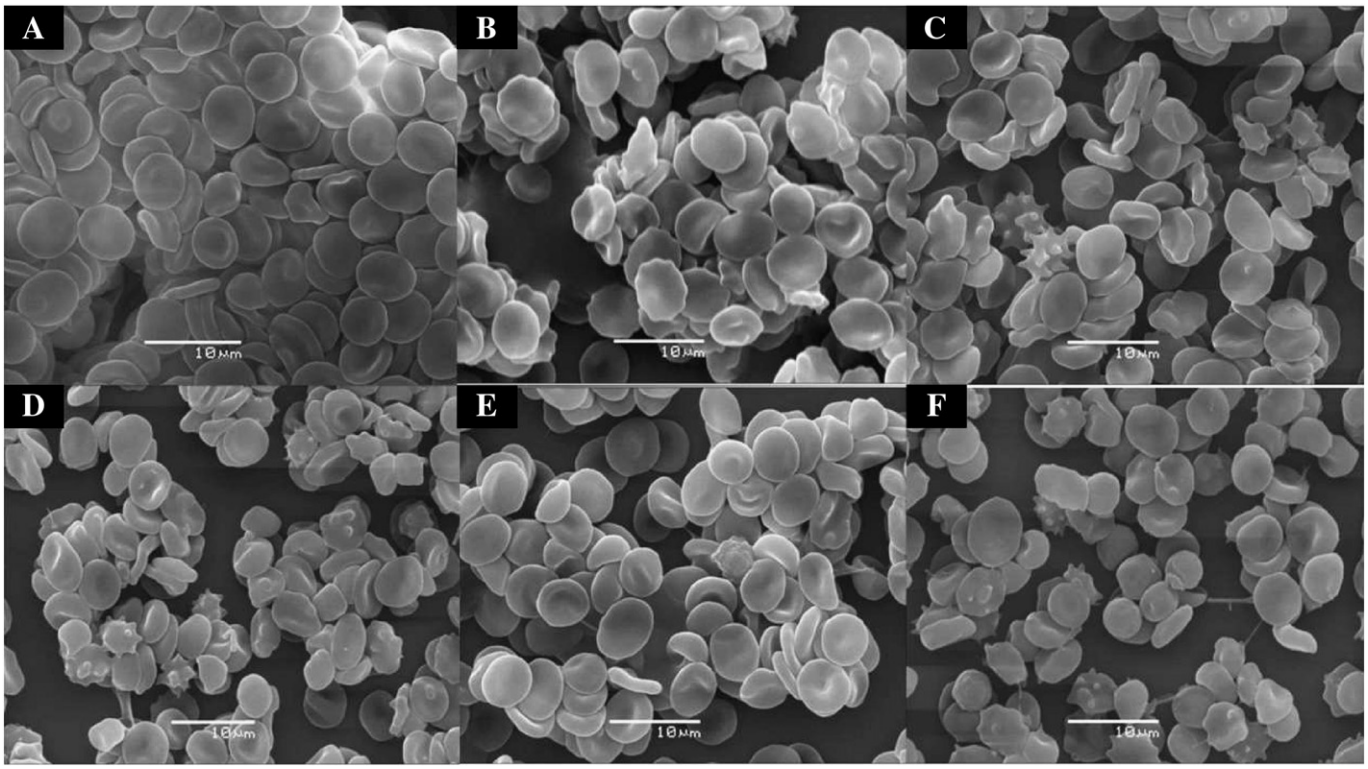

Fig. 6. Effect of M4/HPβCD, M4 and HPβCD on the morphology of human erythrocytes: (A) control; (B) M4/HPβCD 10 μM; (C) M4/HPβCD 100 μM; (D) M4/HPβCD 250 μM; (E) HPβCD 250 μM; (F) M4.

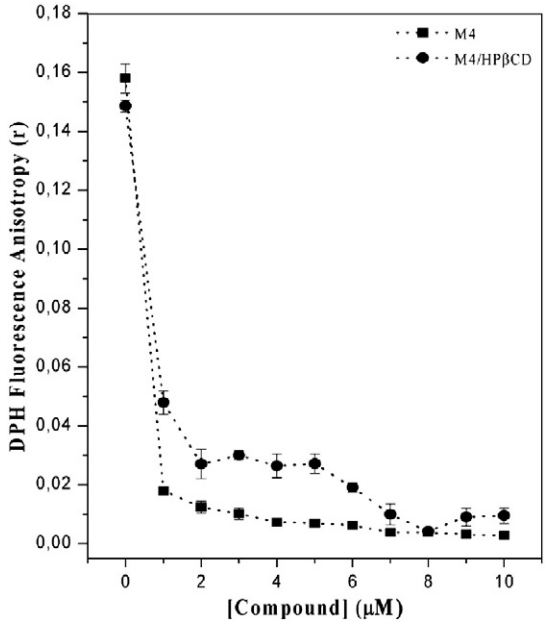

Fig. 8. Effect of M4/HPβCD and M4 on the steady state fluorescence anisotropy of DPH in IUM at 37 °C.

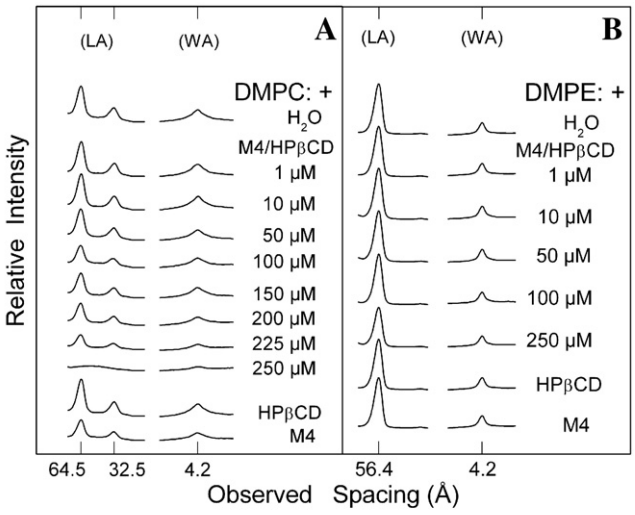

Fig. 10. Microdensitograms from X-ray diffraction patterns of: (A) DMPC and (B) DMPE in water, aqueous solutions of M4/HPβCD, and aqueous suspension of free M4; (LA) and (WA) correspond to low- and wide angle reflections, respectively.

hexagonal packing. Thus, DMPC showed the typical characteristics of the Pβ′ gel phase. Fig. 10A discloses that after exposure to increasing M4/HPβCD concentrations there was a monotonically decrease of DMPC LA and WA reflection intensities, which became negligible at 250 μM. From these results it can be concluded that M4/HPβCD produced a structural perturbation of DMPC bilayers and, as a consequence, a disruption of the in-plane structure and the bilayer stacking. On the other hand, while HPβCD induced a slight increase of DMPC intensities, the opposite effect was detected in the case of free M4. Interestingly, the effect of M4 suspension on DMPC intensities was not as strong as that observed when the quinazoline derivative is complexed, suggesting that cyclodextrin is promoting the interaction of M4 with the bilayer. Results from similar experiments with DMPE, presented in Fig. 10B, show only two reflections: one of 56.4 Å corresponding to the bilayer width, and another of 4.2 Å similar to that observed in DMPC. Additional reflections were not detected with the used set-up. As reported elsewhere, water did not significantly affect the bilayer structure of DMPE [32]. It is possible to observe that increasing M4/HPβCD concentrations did not significantly affect DMPE structure even at the maximum assayed concentration (250 μM). Similarly, neither HPβCD nor M4 induced any structural perturbation to DMPE bilayers.

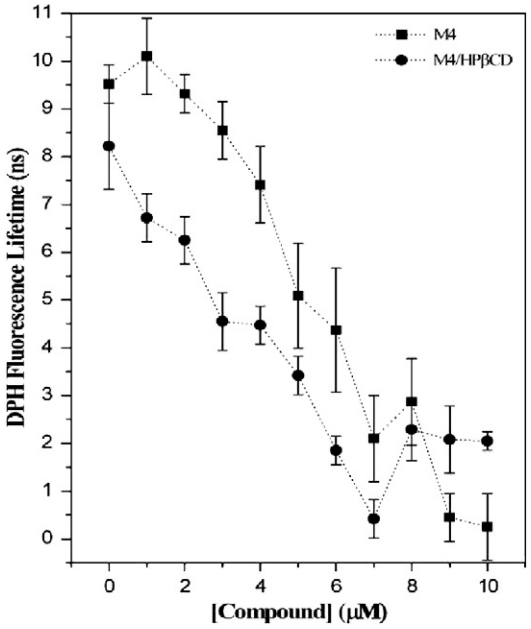

Fig. 9. Effect of M4/HPβCD and M4 on DPH fluorescence lifetime in IUM at 37 °C.

4. Discussion

Although numerous efforts have been made in order to discover novel antimalarial agents and develop novel strategies to overcome resistance, the mode of action and mechanisms of resistance of some of the drugs available today are not fully understood. However, it has been reported that resistance could be related to interactions with biological membranes, interaction with membrane proteins or modifications in the lipid structure [33,34]. Since the pharmacological activity of a molecule frequently involves an initial interaction of the drug with the membrane phospholipids, even if they are not the final target of the drug molecule, and the important role of the erythrocytes host cell membrane on the drug resistance, more investigation about antimalarial drug–membrane interaction is needed. In this paper it is reported the interaction of M4, an antiplasmodial drug complexed with HPβCD, with human red blood cells and molecular models of the erythrocyte membrane. The influence of M4/HPβCD on morphology of intact human erythrocytes was examined by SEM, while IUM were studied by fluorescence spectroscopy. In addition, interactions of M4/HPβCD with DMPC and DMPE lipid bilayers were performed by X-ray diffraction and fluorescence spectroscopy. X-ray crystallography data confirmed the identity of the quinazoline derivative. In order to increase the aqueous solubility of M4 and to avoid the use of organic solvents which could affect the membrane molecular models used in this work, an inclusion complex with HPβCD was prepared. The complex was characterized through ^{1}H NMR data and ESI mass spectrometry, to determine the association type and stoichiometry between M4 and HPβCD respectively; phase-solubility studies indicated that HPβCD enhanced water solubility of M4 through the inclusion complex formation. It is well known that some external factors as well as selective intercalation of foreign species into the outer or inner monolayer of the membrane result in shape changes of the erythrocyte membrane [35–38]. The bilayer-couple hypothesis proposes that crenated shapes (echinocytes) are observed when some agents interact with the outer monolayer while cup-shapes (stomatocytes) are produced when an

interaction takes place in the inner leaflet due to the differential expansion of this membrane monolayer [35].

The results obtained when erythrocytes were incubated in the presence of M4 suspension show that echinocytes were the predominant shape, indicating that the quinazoline derivative might be intercalated in the outer membrane leaflet relative to the inner one. Nonetheless, stomatocytes were also observed (Fig. 6F). An explanation for this finding could be a time-dependent effect: it has been reported that when a molecule initially intercalates into the outer leaflet, causing echinocytosis, it can slowly migrate to the inner leaflet, causing a return to the discocyte structure followed by subsequent stomatocytosis [39]. HPβCD alone also exerted an effect on the normal cell shape; although it cannot be considered drastic, stomatocytes are clearly present in Fig. 6E. Occurrence of these erythrocyte shapes might be partially due to the capacity of CDs to extract cholesterol from cell membranes. β-Cyclodextrin and its derivatives have demonstrated a great capacity to subtract cholesterol from the biological membrane, altering the properties of the lipidic bilayer [40–43]. In addition, it has been reported that depletion of membrane cholesterol promotes stomatocytosis [44]. The inclusion complex M4/HPβCD induced the formation of echinocytes predominantly. This phenomenon can be explained either by the insertion of the inclusion complex in the outer leaflet of the membrane, or by the insertion of M4 delivered from the complex. SEM micrographs also revealed the presence of stomatocytes, explained partially by the effect of the individual components as explained above, or the effect of the M4/HPβCD system.

Fluorescence experiments confirmed SEM results. The observed changes in LUV and IUM were accomplished at lower concentrations than those in which the first changes were evident, in both X-ray diffraction and SEM, demonstrating the great sensitivity of this method. DPH steady state fluorescence anisotropy results, due to its hindered rotational diffusion in the bilayer, indicated that M4 and M4/HPβCD induced a monotonous decrease in the lipid acyl chain packing order at the deep hydrophobic region of DMPC LUVs bilayer (Fig. 7). These changes were substantial in LUV in the gel state (18 °C) and moderate in the liquid crystalline state (37 °C). However, in IUM (Fig. 8), a considerable order decrease occurred mostly upon the first addition of 1 μM of both M4 and M4/HPβCD. The fluorescence lifetime of DPH in a given medium depends on its surrounding dielectric environment provided that no excited state reactions occur. Small alterations in the degree of hydration have been shown to affect significantly the fluorescence lifetime due to fluorophor excited state water interactions [45]. Consequently, fluorescence lifetime measurements can be used to infer changes in the water content of the fluorophor environment. Increasing amounts of the free compound and the complex did not show a significant effect on the DPH lifetime in DMPC LUV at both studied temperatures (data not shown). However, there is a large effect on DPH lifetime in IUM, with a steady decline throughout the concentration range tested (Fig. 9). We suggest that these larger effects on IUM than on fluid phase of DMPC LUVs were due to the presence of lipid–protein interfaces in the erythrocyte membrane. There is considerable evidence that water penetrates into lipid bilayers, at least as far as the glycerol backbone and also deeper between fatty acyl chain packing defects [46]. Lipid–protein interfaces in natural membranes are places of membrane defects, where water is present. It might be that these interfaces are the main locations of both additives inside the membrane. On the other hand, considering that the erythrocyte membrane has high protein content, lipids and proteins must be in close proximity. Thus, all DPH molecules should also be in very close proximity to lipid–protein interfaces. In this context, free M4 and M4/HPβCD induced DPH lifetime decrease in IUM should indicate a hydration increase in the lipid–protein interfaces.

X-ray diffraction performed on bilayers made up of DMPC and DMPE, classes of the major phospholipids present in the outer and inner sides of the erythrocyte membrane agree with those observed in SEM and fluorescence experiments. In fact, they respectively showed that M4/HPβCD disordered the polar head and acyl chain regions of DMPC whereas DMPE bilayers were not affected by M4/HPβCD even at the highest assayed concentration. DMPC and DMPE differ only in their terminal amino groups, these being $^{+}N(CH_3)_3$ in DMPC and $^{+}NH_3$ in DMPE. Moreover, both molecular conformations are very similar in their dry crystalline phases with the hydrocarbon chains mostly parallel and extended, and the polar head groups lying perpendicularly to them [32]. However, the gradual hydration of DMPC results in water filling the highly polar interbilayer spaces with the concomitant increase of their width. This phenomenon allowed the incorporation of M4/HPβCD into DMPC bilayers with the resulting disruption of its structure. On the other hand, DMPE molecules pack tighter than those of DMPC due to their smaller polar groups and higher effective charge, resulting in a very stable bilayer system that is not significantly affected by water. The strong electrostatic interaction and hydrogen bond system also prevented M4/HPβCD from interacting with DMPE and perturbing its structure.

5. Conclusions

PfDHFR inhibitors such as quinazoline derivatives act in the intra-erythrocytic stage of the parasite. To reach this site, drugs have first to interact with erythrocyte membrane. Thus, understanding drug–membrane interaction at molecular level is essential. Present experimental outcomes demonstrated that M4 as an HPβCD inclusion complex interacted with the human erythrocyte lipid bilayer. All results indicated that M4/HPβCD interacted mainly with the outer leaflet of the membrane, where it perturbs the lipid acyl chains ordering and augmented the hydration of the lipid–protein interfaces in the membrane interior where this compound is able to penetrate. Additionally, the results indicate that cyclodextrin facilitated the interaction of M4 with the membrane, a strong reason to consider M4/HPβCD a promising formulation for the treatment of malaria. These results are very valuable because they seem to indicate that alternative modes of interaction of the drug might be operating, starting at the erythrocyte membrane prior to reaching the intracellular target. This in turn could provide key information to tackle the wider issue of drug resistance.

Acknowledgements

We are grateful to José Duguet and Fernando Neira for technical assistance and to Beatriz Quiroz-García for the assistance with NMR spectroscopy. This study was supported by grants from FONDECYT (Project 1090041), UNAM-PAPIIT IN216411, and CONACyT (Ph.D. scholarship 211321 to Y.R.A.).

Appendix A. Supplementary material

CCDC 838592 contains the supplementary crystallographic data for M4. These data can be obtained free or charge from The Cambridge Crystallographic Data Centre via www.ccdc.cam.ac.uk/data_request/cif.

References

[1] http://www.who.int/topics/malaria/en/(Accessed June 2011).
[2] http://www.who.int/malaria/world_malaria_report_2010/en/index.html(Accessed June 2011).
[3] C. Wongsrichanalai, A.L. Pickard, W.H. Wernsdorfer, S.R. Meshnick, Epidemiology of drug-resistant malaria, Lancet Infect. Dis. 2 (2002) 209–218.
[4] E. Ekland, D. Fidock, In vitro evaluations of antimalarial drugs and their relevance to clinical outcomes, Int. J. Parasitol. 38 (2008) 743–747.
[5] D. Fidock, R.T. Eastman, S.A. Ward, S.R. Meshnick, Recent highlights in antimalarial drug resistance and chemotherapy research, Trends Parasitol. 24 (2008) 537–544.
[6] P. Olliaro, Mode of action and mechanisms of resistance for antimalarial drugs, Pharmacol. Ther. 89 (2001) 207–219.
[7] I. Petersen, R. Eastman, M. Lanzer, Drug-resistant malaria: molecular mechanisms and implications for public health, FEBS Lett. 585 (2011) 1551–1562.

[8] J. Davoll, A.M. Johnson, H.J. Davies, Folate antagonists. 2. 2,4-Diamino-6-((aralkyl and (heterocyclic)methyl)amino)quinazolines, a novel class of antimetabolites of interest in drug-resistant malaria and Chagas' disease, J. Med. Chem. 15 (1972) 812–826.
[9] A. Bhattacharjee, M.G. Hartell, D.A. Nichols, R.P. Hicks, B. Stanton, J.E. van Hamont, W.K. Milhous, Structure–activity relationship study of antimalarial indolo [2,1-b] quinazoline-6,12-diones (tryptanthrins). Three dimensional pharmacophore modeling and identification of new antimalarial candidates, Eur. J. Med. Chem. 39 (2004) 59–67.
[10] A. Mishra, K. Srivastava, R. Tripathi, S.K. Puri, S. Batra, Search for new pharmacophores for antimalarial activity. Part III: synthesis and bioevaluation of new 6-thioureido-4-anilinoquinazolines, Eur. J. Med. Chem. 44 (2009) 4404–4412.
[11] P. Verhaeghe, N. Azas, S. Hutter, C. Castera-Ducros, M. Laget, A. Dumètre, M. Gasquet, J.-P. Reboul, S. Rault, P. Rathelot, P. Vanelle, Synthesis and in vitro antiplasmodial evaluation of 4-anilino-2-trichloromethylquinazolines, Bioorg. Med. Chem. 17 (2009) 4313–4322.
[12] Y. Kabri, N. Azas, A. Dumètre, S. Hutter, M. Laget, P. Verhaeghe, A. Gellis, P. Vanelle, Original quinazoline derivatives displaying antiplasmodial properties, Eur. J. Med. Chem. 45 (2010) 616–622.
[13] H.H. Chang, P.K. Dea, Insights into the dynamics of DMSO in phosphatidylcholine bilayers, Biophys. Chem. 94 (2001) 33–40.
[14] H. Dodziuk, Molecules with holes—cyclodextrins, in: H. Dodziuk (Ed.), Cyclodextrins and Their Complexes, Wiley-VCH, 2006, pp. 1–20.
[15] T. Loftsson, D. Hreinsdóttir, M. Másson, Evaluation of cyclodextrin solubilization of drugs, Int. J. Pharm. 302 (2005) 18–28.
[16] T. Loftsson, D. Duchêne, Cyclodextrins and their pharmaceutical applications, Int. J. Pharm. 329 (2007) 1–11.
[17] J.M. Boon, B.D. Smith, Chemical control of phospholipid distribution across bilayer membranes, Med. Res. Rev. 22 (2002) 251–281.
[18] P.F. Devaux, A. Zachawsky, Maintenance and consequences of membrane phospholipids asymmetry, Chem. Phys. Lipids 73 (1994) 107–120.
[19] A.X.S. Bruker, SAINT Software Reference Manual v. 6.23C, Madison, USA, , 2002.
[20] G.M. Sheldrick, SHELXS-97, Crystal Structure Solution, University of Göttingen, Germany, 1990.
[21] G.M. Sheldrick, SHELXL-97, Crystal Structure Refinement, University of Göttingen, Germany, 1997.
[22] E. Baka, J. Comer, K. Takács-Novák, Study of equilibrium solubility measurement by saturation shake-flask method using hydrochlorothiazide as model compound, J. Pharm. Biomed. Anal. 46 (2008) 335–341.
[23] T. Higuchi, K.A. Connors, Phase solubility techniques, Adv. Anal. Chem. Instrum. 4 (1965) 117–212.
[24] J.T. Dodge, C. Mitchell, D.J. Hanahan, The preparation and chemical characteristics of hemoglobin-free ghosts of human erythrocytes, Arch. Biochem. Biophys. 100 (1963) 19–130.
[25] J.R. Lakowicz, Principles of Fluorescence Spectroscopy, Plenum, New York, 1999.
[26] R.D. Spencer, G. Weber, Measurement of subnanosecond fluorescence lifetimes with a cross-correlation phase fluorometer, Ann. N. Y. Acad. Sci. 158 (1969) 361–376.
[27] E. Gratton, D. Jameson, R.D. Hal, Multifrequency phase and modulation fluorometry, Annu. Rev. Biophys. Bioeng. 13 (1984) 105–124.
[28] P.A. Sutton, V. Cody, Conformational analysis of antineoplastic antifolates: the crystal structure of trimetrexate and the aminopterine derivative 4-[N-[(2,4-diamino-6-pteridinyl)methyl]amino]benzoic acid, J. Med. Chem. 30 (1987) 1843–1848.
[29] A. Hempel, N. Camerman, D. Mastropaolo, A. Camerman, The antifolate trimetrexate: observation of the enzyme-binding conformation, Acta Crystallogr. Sect. C. 56 (2000) 1225–1227.
[30] R.A. Rajewski, J.J. Stella, Pharmaceutical applications of cyclodextrins. 2. In vivo drug delivery, J. Pharm. Sci. 85 (1996) 1142–1169.
[31] G. Brecher, M. Bessis, Present status of spiculated red cells and their relationship to the discocyte–echinocyte transformation: a critical review, Blood 40 (1972) 333–344.
[32] M. Suwalsky, Phospholipid bilayers, in: J.C. Salamone (Ed.), Polymeric Materials Encyclopedia, Vol. 7, CRC, Boca Raton, Florida, 1996, pp. 5073–5078.
[33] M. Luxnat, H.J. Galla, Partition of chlorpromazine into lipid bilayer membranes: the effect of membrane structure and composition, Biochim. Biophys. Acta 856 (1986) 274–282.
[34] R.M. Epand, D.S. Lester, The role of membrane biophysical properties in the regulation of protein kinase C activity, Trends Pharmacol. Sci. 11 (1990) 317–320.
[35] M.P. Sheetz, S.J. Singer, Biological membranes as bilayer couples: a molecular mechanism of drug–erythrocyte interactions, Proc. Natl. Acad. Sci. U. S. A. 71 (1974) 4457–4461.
[36] R. Mukhopadhyay, G. Lim, M. Wortis, Echinocyte shapes: bending, stretching, and shear determine spicule shape and spacing, Biophys. J. 82 (2002) 1756–1772.
[37] K.D. Tachev, K.D. Danov, P.A. Kralchevsky, On the mechanism of stomatocyte–echinocyte transformations of red blood cells: experiment and theoretical model, Colloids Surf. B. 34 (2004) 123–140.
[38] G. Lim, M. Wortis, R. Mukhopadhyay, Stomatocyte–discocyte–echinocyte sequence of the human red blood cell: evidence for the bilayer–couple hypothesis from membrane mechanics, Proc. Natl. Acad. Sci. U. S. A. 99 (2002) 16766–16769.
[39] B. Isomaa, H. Hägerstrand, G. Paatero, Shape transformations induced by amphiphiles in erythrocytes, Biochim. Biophys. Acta 899 (1987) 93–103.
[40] T. Kiss, F. Fenyvesi, I. Bácskay, R. Iványi, J. Váradi, E. Fenyvesi, L. Szente, A. Tósaki, M. Vecsernyés, Evaluation of the cytotoxicity of β-cyclodextrin derivatives: evidence for the role of cholesterol extraction, Eur. J. Pharm. Sci. 40 (2010) 376–380.
[41] T.L. Steck, J. Ye, I. Lange, Probing red cell membrane cholesterol movement with cyclodextrin, Biophys. J. 83 (2002) 2118–2125.
[42] J. Szejtli, T. Cserháti, M. Szögyi, Interactions between cyclodextrins and cell–membrane phospholipids, Carbohydr. Polym. 6 (1986) 35–49.
[43] Y. Ohtani, T. Irie, K. Uekama, K. Fukunaga, J. Pitha, Differential effects of α, β- and γ-cyclodextrins on human erythrocytes, Eur. J. Biochem. 186 (1989) 17–22.
[44] Y. Lange, J.M. Slayton, Interaction of cholesterol and lysophosphatidylcholine in determining red cell shape, J. Lipid Res. 23 (1982) 1121–1127.
[45] C. Zannoni, A. Argioni, P. Cavatorta, Fluorescence depolarization in liquid crystals and membrane bilayers, Chem. Phys. Lipids 32 (1983) 179–250.
[46] C. Ho, C.D. Stubbs, Hydration at the membrane protein–lipid interface, Biophys. J. 63 (1992) 897–902.